Peer-reviewed version available at *Catalysts* **2020**, *10*, 190; doi:10.3390/catal10020190

Sustainable Biodiesel Synthesis from Honne-Rubber-Neem Oil Blend with a Novel Mesoporous Base Catalyst Synthesized from a Mixture of Three Agrowastes

Olayomi A Falowo[1,#], Omoniyi Pereao[2], Tunde V Ojumu[2], Eriola Betiku[1,3,*]

[1]Biochemical Engineering Laboratory, Department of Chemical Engineering, Obafemi Awolowo University, Ile-Ife 220005, Osun State, Nigeria.

[2]Department of Chemical Engineering, Cape Peninsula University of Technology, Bellville 7535, Symphony Way, Bellville, Cape Town, South Africa.

[3]Department of Biological Sciences, Florida Agricultural and Mechanical Engineering University, Tallahassee, Florida 32307, USA.

[#]Present address: Department of Chemical Engineering, Landmark University, Omu-Aran, Kwara State, Nigeria.

*Email Address of Corresponding Author: eriola.betiku@famu.edu, ebetiku@yahoo.com

Peer-reviewed version available at *Catalysts* **2020**, *10*, 190; doi:10.3390/catal10020190

Abstract

Application of solid catalysts synthesized from agricultural wastes provides an environmentally benign and low-cost process route to synthesis of biodiesel. An ash containing equal mixture of cocoa pod husk, plantain peel and kola nut pod husk ashes (CPK) which was obtained by open combustion of each of the biomass in air and calcined at 500 ^{o}C for 4 h. The calcined CPK ash was characterized to determine its catalytic potential. Two-level transesterification technique was used to synthesize biodiesel using the developed catalyst. The process parameters involved were optimized for the microwave-aided transesterification of a blend of honne, rubber seed and neem oils in volumetric ratio 20:20:60, respectively. The study showed that the ash derived from combination of the biomass wastes provided a catalyst which consists all necessary catalytic ingredients in their relative abundance. The calcined CPK consists of 47.67% of potassium, 5.56% calcium and 4.21% magnesium attesting to its heterogenous status. The physisorption isotherms reveals that it was dominantly mesoporous in structure made up of nanoparticles. Maximum of 98.45 wt.% biodiesel was obtained through MeOH:oil blend of 12:1, CPK concentration of 1.158 wt.% and reaction time of 6 min under microwave irradiation. Quality of the synthesized biodiesel satisfied the requirements stipulated by standard specifications. Thus, this work demonstrates that blend of agrowastes and mixture of non-edible oils could be used to synthesize quality and sustainable biodiesel that can replace fossil diesel.

Keywords

Heterogenous catalyst, biodiesel, agrowaste, microwave, optimization, transesterification.

Peer-reviewed version available at *Catalysts* **2020**, *10*, 190; doi:10.3390/catal10020190

Graphical abstract

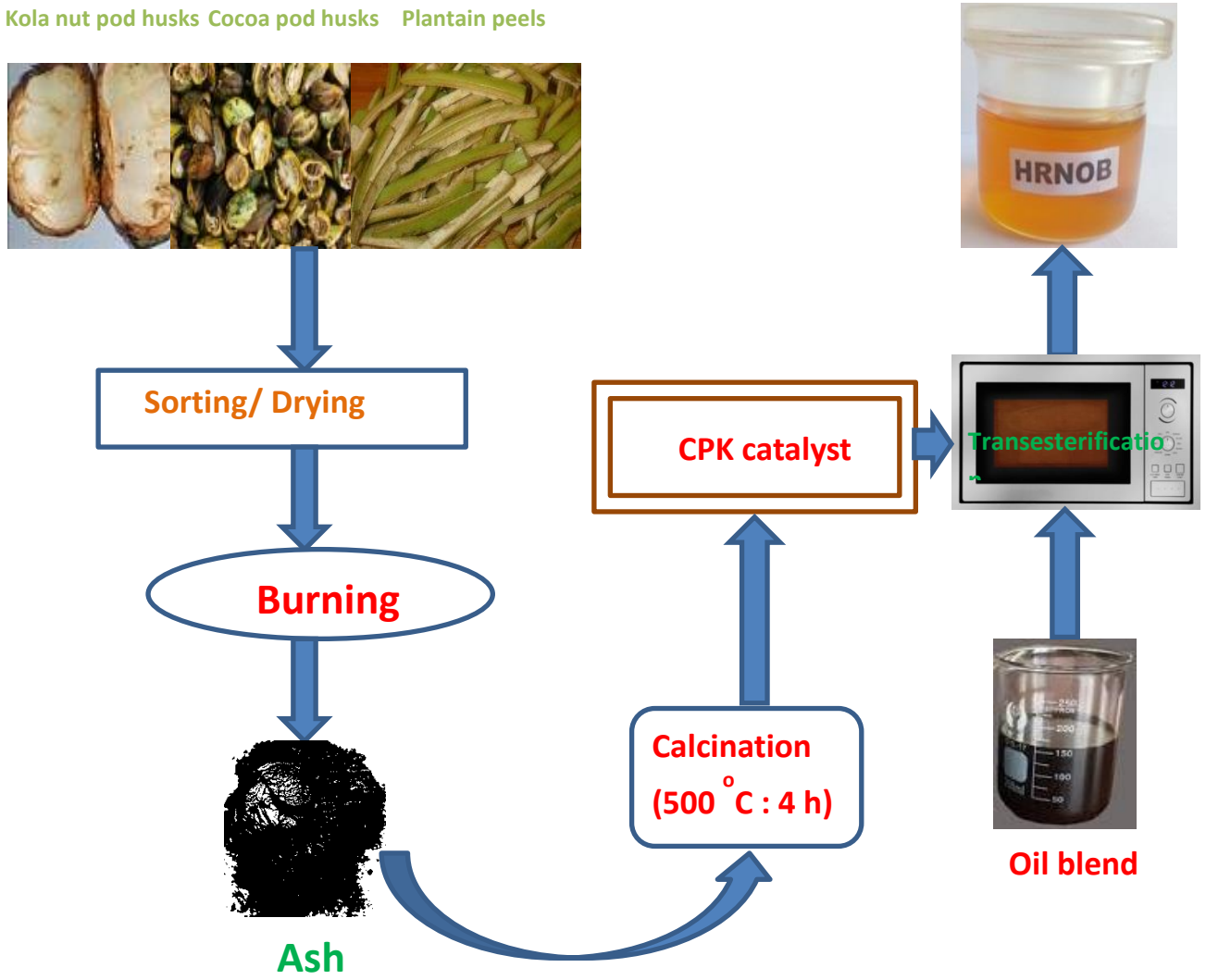

Peer-reviewed version available at Catalysts 2020, 10, 190; doi:10.3390/catal10020190

1 Introduction

Active research in renewable and nonpolluting energy sources has taken center stage in a bid to enhance energy security and prevent environmental degradation. Presently, fuel derived from fossil sources is the socioeconomic mainstay of several countries in the world. However, concerns such as unstable petroleum price, depletion of oil reserve and emission of greenhouse gases are discouraging long-term usage of petro-diesel worldwide [1]. Total or partial replacement of fossil-derived fuel with clean, economically feasible, sustainable and renewable energy sources has become imperative towards achieving balance in energy security and environmental protection in any developing economy.

Biodiesel is a renewable fuel having remarkable features and can serve as an alternative to fossil diesel. Transesterification of triglycerides in vegetable oil or animal fat or lipids from algae and methanol or ethanol in the presence of a catalyst is by far the most applied technique for biodiesel synthesis. Generally, biodiesel synthesis via transesterification employs catalyst that can be acid, alkali or enzyme [2]. Free fatty acid (FFA) level in oils primarily determines the choice of catalyst to be used for the process [3]. Homogeneous catalysis and heterogeneous catalysis have been applied to transesterification of oils to obtain biodiesel.

Homogeneous catalysis has several advantages including low price, abundant raw materials, shorter reaction time, high catalytic activities and moderate operating conditions [4, 5]. In spite of these benefits, homogeneous catalysis is not without shortcomings which limits its continuous application in biodiesel production. Homogenous alkali catalysts are highly hygroscopic; they absorb water during storage [5]. Besides, purification steps require several washing and removing the traces of Na/K together with the glycerol from the biodiesel becomes increasingly difficult. Lot of water required in washing and consequent wastewater treatment cost leads to high production cost [6]. To counter these negative effects posed by this type of catalysts, eco-friendly materials are used to synthesize heterogenous solid catalyst [7, 8]. Heterogenous catalysis offers several advantages including recyclability, easy separation, non-corrosive, higher selectivity, environmental benign and longer catalyst life [4, 5]. Exploitation of wastes for catalyst development in biodiesel production could be used to mitigate environmental damage [9, 10]. Currently, lot of effort has been put into development of heterogeneous solid acid and alkali catalysts for biodiesel synthesis which may help reduce overall production cost. Evidence from several works indicate that it has been successfully applied for biodiesel production. Sources of biomass-derived catalysts include waste shell, biomass ashes, activated carbon supported catalyst, animal bones and waste coral [10-15].

Peer-reviewed version available at Catalysts 2020, 10, 190; doi:10.3390/catal10020190

The belief that heterogenous catalyst is limited by mass transfer rate, low active site and leaching may have been exaggerated and attaching solid catalyst to support will increase the price of biodiesel. It should be noted that catalyst loaded on support incurred extra cost, thereby further increasing production cost. In contrast, biodiesel production using different heterogenous alkali catalysts prepared by calcination without catalyst support showed high yields. For instance, conversion of soybean oil to biodiesel at temperature of 65 ^{o}C, reaction time of 25 min, MeOH:oil of 12:1 and catalyst amount of 7 wt.% from waste *Brassica nigra* plant gave 98.79 wt.% yield [13]. Betiku *et al*. [7] reported biodiesel yield of 98.5 wt.% using calcined banana peel as catalyst at the reaction condition of temperature of 65 ^{o}C, time of 69.02 min, MeOH:oil of 7.6:1 and catalyst amount of 2.75 wt.% from Napoleon's plume oil. Biodiesel produced from *Ceiba pentandra* oil gave a maximum yield of 98.69 ± 0.18 wt.% using calcined banana peduncle ash of 1.978 wt.% at reaction temperature of 65 ^{o}C, time of 1 h and MeOH:oil of 9.20:1 [14]. Transesterification of soybean oil in the presence of banana peel ash at room temperature, reaction time of [14], MeOH:oil of 6:1 and catalyst amount of 0.7 wt.% gave biodiesel yield of 98.95% [16[16]. Several heterogenous catalysts with high catalytic activities have been developed at suitable calcination temperatures from waste materials. Calcination of ash is a cost-effective approach in producing catalyst [9]. Although carbon-based solid catalysts have been touted as the ideal catalyst for transesterification process; cost incurred due to high carbonization temperature and unwanted chemical reaction due to functionalization of the carbonaceous substance restricted its application on a large scale. Hence, calcination of biomass ashes could offer a simpler and cost-effective means in synthesizing catalyst with high catalytic behavior for transesterification processes.

Proximate analysis has revealed that agricultural wastes such as kola nut pod husk, plantain peel (ripe and unripe) and cocoa pod husk are potential raw materials for industrial applications [17]. Heterogeneous biobase catalyst has been synthesized separately from kola nut pod husks [18, 19], cocoa pod husks [20, 21] and plantain peels [22, 23] for the conversion of vegetable oils to biodiesel (Table 1). But the catalytic activity of the ash obtained from the mixture of these wastes as a potential biobase catalyst for the transesterification reaction has not been reported. Mixtures of oils *viz*. edible, inedible and waste cooking oils have been exploited for biodiesel synthesis. Menegehetti *et al*. [24] evaluated mixtures of cottonseed/castor oils (50:50) and soybean/castor (25:75) oils for biodiesel synthesis and reported 86 and 87 wt.% yields, respectively. Khalil *et al*. [25] produced biodiesel from a blend of palm oil/rubber seed oil (50:50) and obtained 97 wt.% yield.

Peer-reviewed version available at *Catalysts* **2020**, *10*, 190; doi:10.3390/catal10020190

Table 1. Solid based-heterogeneous catalyst derived from biomass

Biowaste	Calcination condition			Transesterification condition					Biodiesel yield	Reference
	Heat (°C)	Time (h)	Main metallic content	Oil	MeOH:oil molar ratio	Catalyst (wt.%)	Temperature (°C)	Time (min)		
Cocoa pod husk	700	4	K (59.2%), Mg (3%)	Neem	0.73v/v	0.65	65	57	99.3	[21]
Cocoa pod husk	650	4	-	Soybean	6:1	1	60	120	91.4	[20]
Plantain peel (ripe)	700	4	K (51.02%), Mg (1.15%)	Neem	0.73v/v	0.65	65	57	99.2	[23]
Plantain peel (unripe)	500	3.5	K (54.73%), Ca (1.13%), Al (3.42%)	Yellow oleander	0.33v/v	3	60	90	95.25	[22]
Kola nut husk	500	4	K (47.14%), Ca (7.59%), Mg (5.32%)	Kariya	6:1	3	65	75	98.67	[18]
Kola nut husk	600	3	K (47.14%), Ca (7.59%), Mg (5.32%)	Yellow oleander	6:1	1.5	60	90	84.5	[19]
Banana peel	700	4	K (99.73%), Ca (0.03%), Na (0.19%), Mg (0.03%), Fe (0.01%)	Napoleon's plume	7.6:1	2.75	65	69.02	98.5	[7]
Banana peel	Open air burning	NS	K (70.06%), Ca (9.54%) Mg (1.78%), Fe (1.49%)	Soybean	6:1	0.7	Room temperature	240	98.95%	[16]
Banana peduncle	700	4	K K (68.37%), Mg K (4.66%), Ca K (7.09%)	*Ceiba pentandra*	9.20:1	1.978	60	60	98.69%	[14]
CPK	500	4	K (47.67%), Ca (5.56%), Mg (4.21%)	Neem-rubber-honne oil blend	12:1	1.16	150 W	6	98.45	Present study

Peer-reviewed version available at Catalysts 2020, 10, 190; doi:10.3390/catal10020190

Also, mixture of pongamia/neem oils (70:30) was converted to biodiesel with a yield of 86.3 wt.% [26]. In the study of mixture of waste cooking/honne oils (70:30) carried out with the aid of a microwave, a yield of 97.65 wt.% was reported by Milano et al. [27]. In the work of Miraculas *et al*. [28], mixture of pongamia/jatropha/honne oils (in equal proportions) was used to produce biodiesel with a reported yield of ~98 wt.%. When mixture of soybean oil and rapeseed oil (50:50) was used as feedstock for biodiesel synthesis by Qiu et al. [29], a yield of ~94% was observed using KOH of 0.8 wt.%, temperature of 55 ^{o}C, MeOH:oil blend of 5:1 and time of 2 h. In our previous report with mixture of rubber seed/neem oils (40:60), 98.77 wt.% biodiesel yield was achieved under transesterification aided with microwave irradiation [30]. Fadhil et al. [31] obtained 95.2 ± 2.5 wt.% biodiesel yield when castor seed oil and waste fish oil were mixed together (50:50) using MeOH:blend oil of 8:1, KOH of 0.5 wt.%, time of 30 min, stirring rate of 600 rpm and temperature of 32 ^{o}C. All of these reports synthesized biodiesel through transesterification process with either KOH or NaOH as the homogeneous catalyst except in our work in which calcined ash of elephant ear pod husk was used as a base catalyst. Besides the work of Milano *et al*. [27] and Falowo *et al*. [30], all the other works did not apply microwave irradiation which accounts for the longer time needed to complete the transesterification reaction.

The focus of this present study is to synthesize a functional heterogeneous base catalyst from a mixture of cocoa (*Theobroma cacao*) pod husk, plantain (*Musa paradisiaca*) peel and kola nut (*Cola nitida*) pod husk (CPK) and apply it to transesterification of a ternary blend of inedible oils made up of honne (*Calophyllum inophyllum*), neem (*Azadirachta indica*) and rubber seed (*Hevea brasiliensis*) under microwave-assisted transesterification. This was with a view to developing a sustainable path for biodiesel production to deal with both food *vs* fuel concerns and environmental threat. Detail characterization of the catalyst developed was carried out to ascertain it catalytic potential. The important process parameters for the transesterification process were optimized to maximize biodiesel yield from the oil blend.

2. Results and discussion

2.1. Calcined CPK characterization

EDX results on CPK

Table 2 describes the elemental composition of the analyzed samples of calcined CPK carried out at various temperatures. The major metals present are K, Ca and Mg (Figure 1). From the results, variation of calcination temperature affected the element present and amount of each element as previously established [21]. Metals such as K, Ca, Mg are good metals for

Peer-reviewed version available at Catalysts 2020, 10, 190; doi:10.3390/catal10020190

catalyst formation because of their ability to easily donate electron to other molecules. At 500 °C and 700 °C, K had the highest peak of 47.67% and 47.93%, respectively among the elements present. Also, Mg and Ca are present in higher amounts at 500 °C than at 700 °C. Increasing the calcination temperature beyond 700 °C led to slight reduction in K content, this could possibly be attributed to the vaporization of KCl [32]. On the basis of this observation, coupled with the conservation of energy by lowering calcination temperature, more CPK production was subsequently carried out at 500 °C.

Table 2. Elemental composition of calcined CPK by EDX

	Composition (%)									
Temperature (°C)	O	Mg	Si	P	S	Cl	K	Ca	Fe	Al
300	40.43	4.06	0.90	1.74	1.41	1.97	43.99	5.50	0.00	0.00
500	37.21	4.21	0.56	1.65	1.26	1.88	47.67	5.56	0.00	0.00
700	41.20	3.05	0.79	1.61	0.92	1.88	47.93	3.93	0.00	0.00
900	41.59	1.85	1.41	1.77	1.29	1.43	45.55	4.68	0.64	0.00
1100	45.30	0.81	2.82	5.20	1.17	1.03	43.90	0.00	0.00	0.75

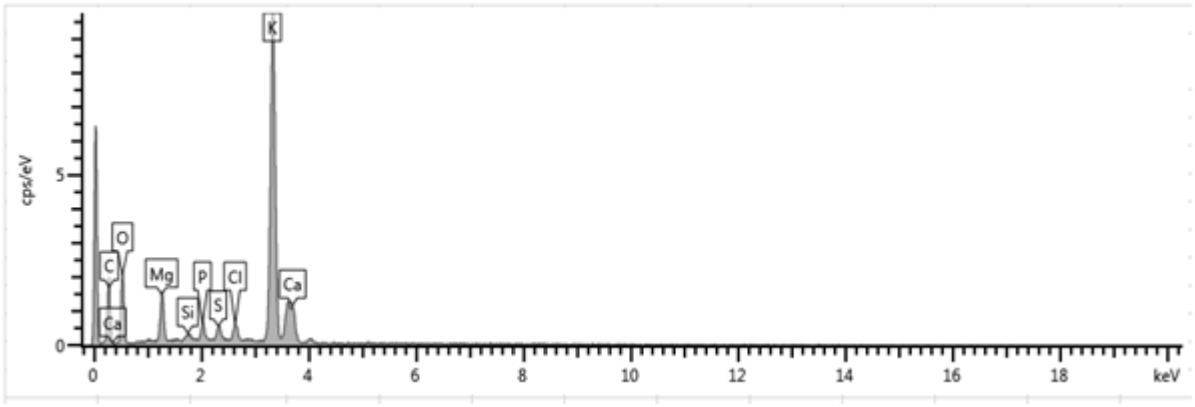

Figure 1. EDX plot of calcined CPK ash.

Results in this study agree with previous reports. As can be seen in Table 1, K has been observed to be the dominant element in calcined cocoa pod husk ash [20], calcined plantain peel [22] and calcined kola nut pod ash [18, 19]. In another report, mass fraction of calcined banana peduncle ash at 700 °C for 4 h showed K (68.37%) as the dominant component but with traces of Ca and Mg too [14]. Gohain *et al*. [15] reported that calcined *Carica papaya* stem at 700 °C for 4 h contains K (56.71%), Ca (21.08%), Na (14.78%) and Mg (4.41%). Calcined waste of cupuaçu seeds at 800 °C for 4 h was reported to contain K, Ca and Mg with composition of 54.76, 17.57 and 3.61%, respectively [12]. Also, it was found that K (56.13%) and Ca (26.04%) were the predominant elements in *Brassica nigra* leaves calcined at 550 °C

Peer-reviewed version available at Catalysts 2020, 10, 190; doi:10.3390/catal10020190

for 2 h [13]. All of these calcined ashes from agricultural wastes have been tested as catalysts for transesterification reactions to synthesize biodiesel with great success.

SEM analysis of calcined CPK

Morphological nature of the calcined CPK shows small aggregates of fine particles (Figure 2). The image is porous and spongy in nature with cluster of small particles scattered in the micrograph. It is worth mentioning that the sintering of metal oxide could be responsible for the agglomerated particles at the calcined temperature [30]. Particle structure of this nature usually exhibits a higher surface area, thereby suggesting a good catalytic activity of the developed catalyst. The SEM image reveals irregular particle size of uneven shape. Observation of similar structure of ashes developed from cocoa pod husk [21], ripe plantain peel [23], unripe plantain peel [22] and kola nut pod husk [18] have been reported.

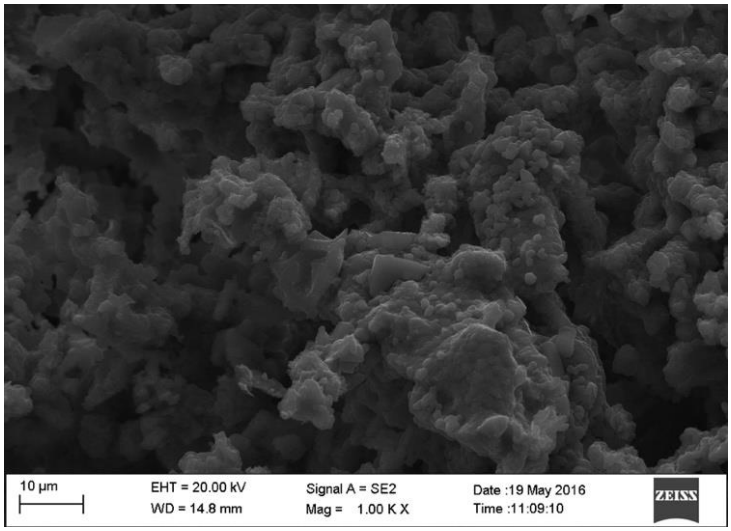

Figure 2. SEM image of calcined CPK ash

XRD pattern of calcined CPK

The crystalline structure of the calcined CPK was described by XRD diffractogram (Figure 3). The diffraction peak centered at 2θ shows numerous peaks which is an indication of crystalline phases. Calcination led to the decomposition of the compounds present in the CPK to KCl, $K_2CO_3 \cdot 1.5H_2O$ and $K_2Ca(CO_3)$. The XRD spectrum shows that potassium compounds dominated the phases. The observation agrees with the elemental composition obtained by the EDX analysis supporting that K is the predominant element in the CPK. Furthermore, our observation aligns with earlier reports on the calcined individual agrowastes

Peer-reviewed version available at Catalysts 2020, 10, 190; doi:10.3390/catal10020190

which was combined in this study [18, 21-23]. This is also true for agrowastes such as banana peduncle and *C. papaya* stem [14, 15].

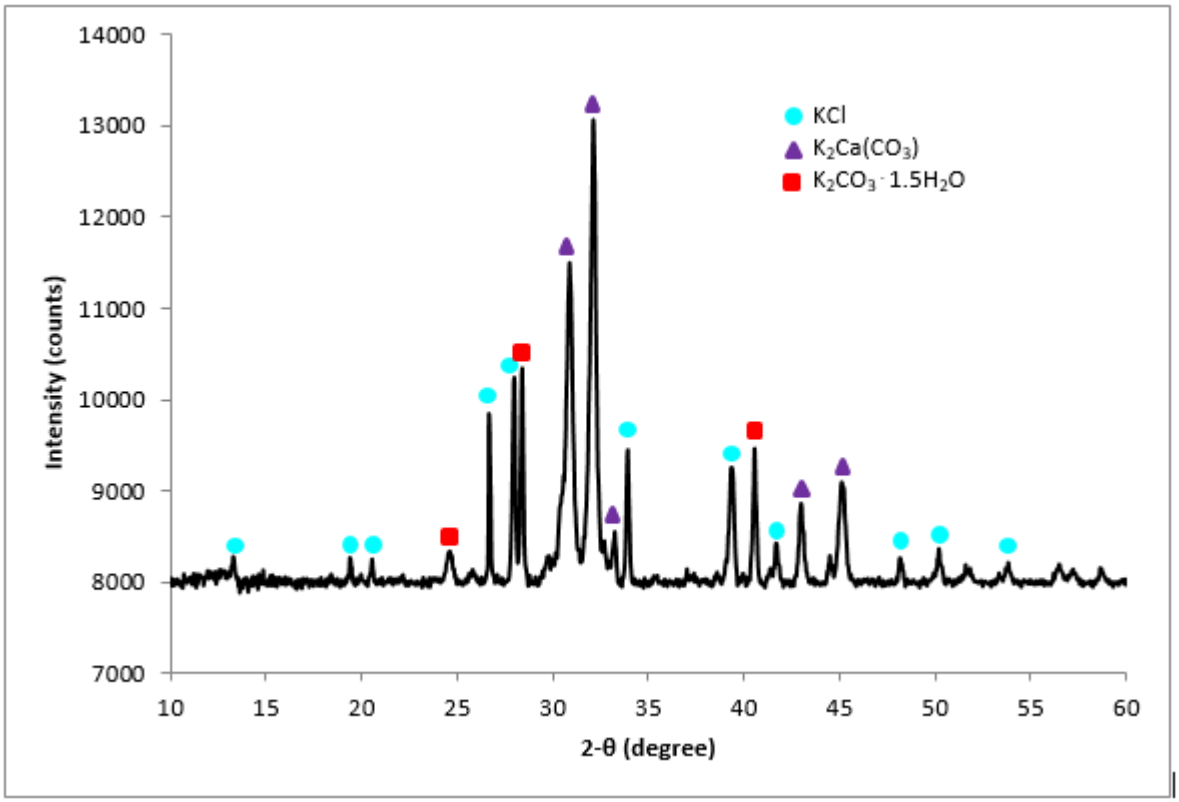

Figure 3. XRD plot of calcined CPK ash.

IR spectrum for calcined CPK

The IR spectrum of calcined CPK is shown in Figure 4. A close observation shows that adsorption bands at 1367 and 879 cm^{-1} indicate the presence of carbonate which depicts stretching and bending of C-O vibration [33]. Also, -C-O stretching and bending vibrations of carbonate was detected at 1132 cm^{-1} [13]. The phosphate and silicate ion components are identified in the adsorption band of 1029 cm^{-1} [7, 13, 23]. The band at 679 cm^{-1} is attributable to stretching vibration of K-O [15]. The characteristics band at 879 and 679 cm^{-1} indicate the presence of K_2CO_3 $1.5H_2O$. In addition, the characteristics band at 1367 cm^{-1} in calcined CPK ash is prominent for K_2CO_3 [7, 34]. This band is also supported by the strong presence of K_2CO_3 in the XRD spectrum of calcined CPK (Figure 3). The EDX results (Table 2) corroborate the observed functional groups identified in the IR spectrum of the CPK. Previous studies on the synthesis of solid catalysts from cocoa pod husk [21], plantain peel [22, 23] and kola nut pod husk [18], precursors of the calcined CPK, show that their spectral have similar

Peer-reviewed version available at Catalysts 2020, 10, 190; doi:10.3390/catal10020190

functional groups to the IR in this study. In addition, these compounds have been reported in calcined ashes of *Brassica nigra* leaves [13], *C. papaya* stem [15] and elephant ear pod husk [30].

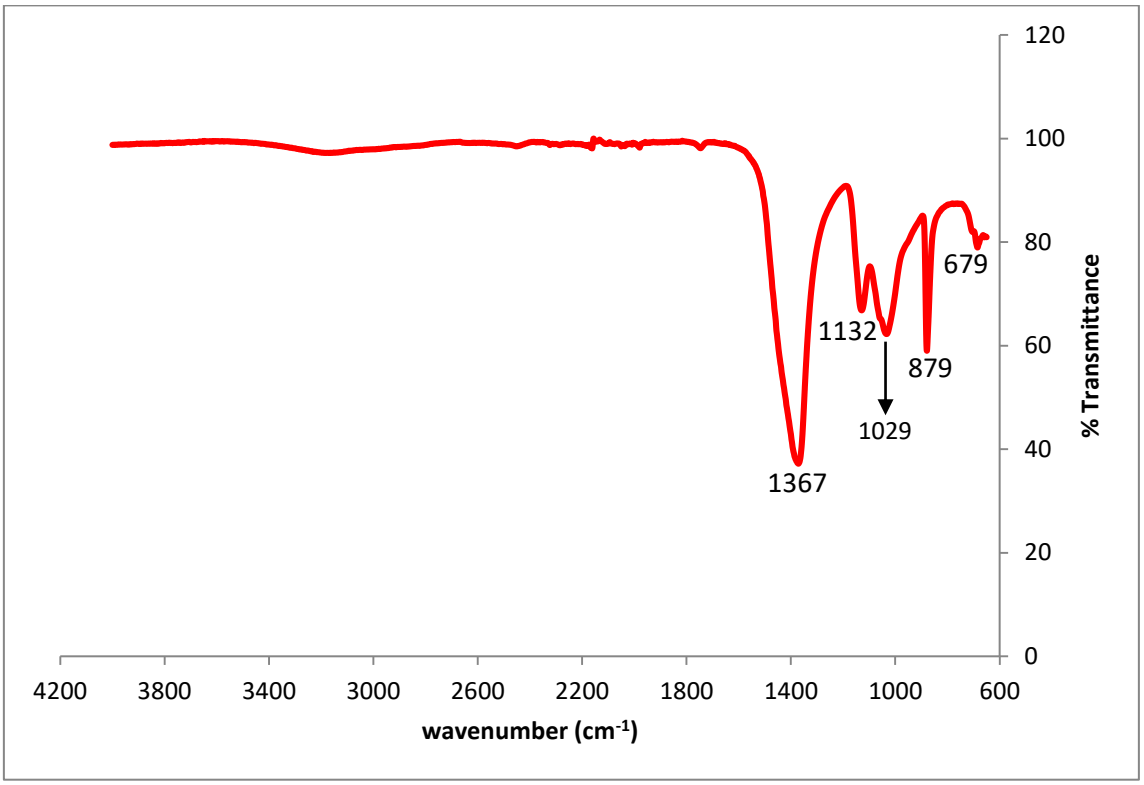

Figure 4. FTIR spectrum of calcined CPK ash

Surface properties of calcined CPK

Measurable quantities such as pore volume and specific surface area that described physical properties of the calcined CPK at 500 ^{o}C were determined by physisorption of nitrogen gas (N_2) at 77.3 K. The calcined CPK had BET surface area of 16.871 m^2/g and the BJH pore volume was 0.041 cm^3/g. The BET surface areas reported for calcined ashes of cocoa pod husk, plantain peel and kola nut pod husk are 2.76, 18.80 and 5.22, respectively [18, 21, 23]. This shows that combing the agrowastes has improved the surface areas of both calcined ashes of cocoa pod husk and kola nut pod husk. The surface area of the calcined CPK ash in this present study is much higher compare to calcined ashes of *Brassica nigra* leaves, *Musa acuminata* peel and wood obtained from *Acacia nilotica* with 7.038, 1.4546 and 1.33 - 3.72 m^2/g, respectively [13, 16, 32]. The physisorption isotherms of the calcined CPK ash is depicted in Figure 5. At low P/P_o, the adsorption isotherm shows progressive increase in the volume of N_2 adsorbed, an

Peer-reviewed version available at Catalysts 2020, 10, 190; doi:10.3390/catal10020190

important feature in type IV isotherm [35, 36]. A sharp uptake in adsorbate volume observed at $P/P_o > 0.9$ can be linked to adsorption in the mesopores region of the catalyst together with type *H3* loop, an indication of the presence of mesopores that consists of agglomerates in the calcined CPK [30, 35-37]. The plot of the BJH pore-size distribution for the calcined CPK is illustrated in Figure 6. The plot suggests the presence of nanoparticles of mesopore size (2 - 50 nm) for the calcined CPK ash [35].

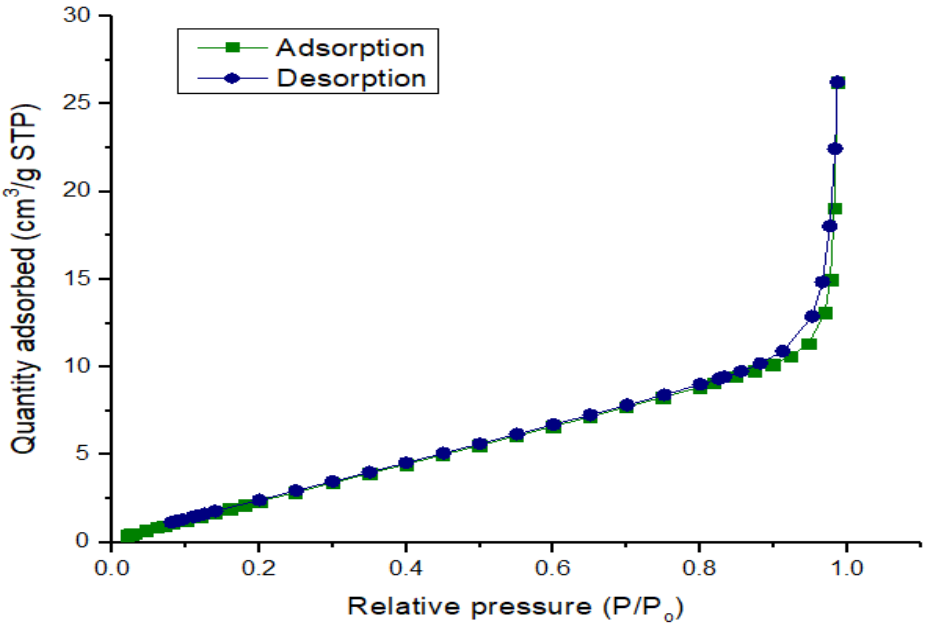

Figure 5. Plot of physisorption isotherms against relative pressure.

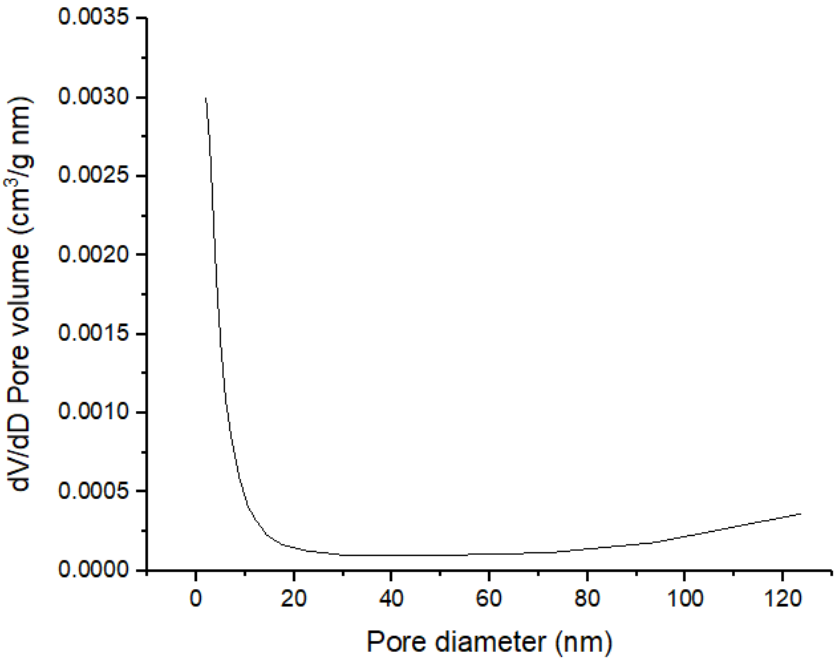

Figure 6. Pore size distribution of calcined CPK ash.

Peer-reviewed version available at *Catalysts* **2020**, *10*, 190; doi:10.3390/catal10020190

2.2. Physicochemical properties of oil blends

The suitability of the oil blend for biodiesel synthesis was determined by evaluating the physicochemical properties of each oil blend samples obtained from crude honne, rubber seed and neem oils. Based on the properties of the oil blends presented in Table 3, acid value was extremely high for all oil blends with H20R20N60 having the lowest. The value increases with decrease in the proportion of neem oil in the oil blend. Oil density varies based on the nature of the triglycerides [38]. In this study, the density of the oil blend increases with increase in the amount of neem oil but decrease with the increase in rubber seed oil. Changes in kinematic viscosity across the blend follow the same pattern as that of density since both have a linear correlation [39]. Kinematic viscosity was lowest when the honne oil had highest proportion. Iodine value increased as the proportion of rubber seed oil increased in the blends while the value decreased as the proportion of neem oil in the mixture increased. Though, calorific value of all blends was high, particularly when honne and neem oils are high in the mixture, however, there was an appreciable increase in H20R20N60 (code named HRNO). Therefore, properties such as lower saponification value, acid value, iodine value and high calorific value made HRNO blend a suitable choice for the biodiesel conversion.

Table 3. Physicochemical properties of hone-rubber seed-neem oil blends

Properties	H20R60N20	H40R40N20	H60R20N20	H20R40N40	H40R20N40	H20R20N60	H33R33N33
RI	1.4726 ± 0	1.4732 ± 0	1.4743 ± 0	1.4738 ± 0	1.4745 ± 0.02	1.4732 ± 0.01	1.4737 ± 0
Density (g/cm^3)	0.931 ± 0.01	0.93 ± 0.02	0.934 ± 0.2	0.935 ± 0.94	0.935 ± 0.01	0.938 ± 1.34	0.934 ± 0.01
Viscosity (mm^2/s)	51.31 ± 1.67	49.06 ± 0.78	47.99 ± 0.99	65.08 ± 0.22	57.48 ± 1.15	66.15 ± 2.08	59.1 ± 0.18
Acid Value (mg KOH/ g)	55.68 ± 2.2	47.01 ± 0.11	41.4 ± 0.11	42.53 ± 0.12	35.35 ± 0.12	31.97± 0.11	39.5 ± 0.46
IV (g I_2/100g oil)	90.62 ± 2.4	85.76 ± 1.46	87.72 ± 1.46	84.84 ± 2.46	82.38 ± 1.94	81.89 ± 2.42	83.4 ± 0.99
SV (mg KOH/g)	219.49 ± 0.70	236.32 ± 0.70	244.04 ± 0.34	254.55 ± 0.70	241.94 ± 0.61	206.17 ± 1.40	224.4 ± 0 .48
Calorific value (MJ/kg)	39.07 ± 0.07	38.4 5± 0.05	38.11 ± 0.01	37.73 ± 0.06	38.26 ± 0.04	39.75 ± 0.02	39 ± 0.01

RI – refractive index, IV – iodine value, SV – saponification value, value. Values reported are mean with standard deviation of triplicate determinations.

2.3. Results of esterification of HRNO

The pretreatment step, which is an esterification reaction, was included to reduce the acid value of the HRNO to < 2 mg KOH/g oil or %FFA < 1, so as to avoid soap formation during transesterification process. The results obtained showed a significant reduction in %FFA from 16.07 to a final value of 0.88 ± 0.085 using reaction time of 120 min, temperature of 65 ^{o}C, MeOH:oil blend of 25:1 and catalyst weight of 10 wt.%. The result shows the good catalytic capability of the ferric sulfate in addition to easy separation and recovery of the catalyst [40]. Similar reduction of %FFA was reported at the same processing condition

Peer-reviewed version available at Catalysts 2020, 10, 190; doi:10.3390/catal10020190

using a blend of rubber seed oil and neem oil. Hence, the process condition was used for the mass production of esterified HRNO used for the transesterification step.

2.4. Modelling results of transesterification process

The central composite rotatable design (CCRD) modeling of the transesterification of HRNO via irradiation with microwave was carried out. The regression model equation obtained is described by the Eq. (1).

$$HRNOB = +87.89 + 2.08A - 0.50B + 1.10C + 1.67AB + 3.22AC - 4.57BC - 1.59A^2 + 0.52B^2 + 0.63C^2 \quad (1)$$

where, HRNOB (wt.%) is the response from the oil blend, the terms *A*, *B* and *C* represent MeOH:HRNO, CPK concentration (wt.%) and reaction time (min), respectively. *AB*, *AC*, and *BC* are the interaction terms, and A^2, B^2, and C^2 are the quadratic terms of the independent variables.

ANOVA results and regression analysis of the selected responses are presented in Table 4 to establish the level of significance of the model as well as all the terms of the model.

Table 4. Statistics results for the model

Source of variance	Sum of Squares	Degree of freedom	Mean Square	F Value	p-value
Model	282.08	9	31.34	87.33	< 0.0001
A- MeOH:HRNO	17.29	1	17.29	48.17	0.0010
B- CPK loading	0.99	1	0.99	2.77	0.1569
C- Time	4.87	1	4.87	13.56	0.0143
AB	5.60	1	5.60	15.60	0.0109
AC	20.69	1	20.69	57.65	0.0006
BC	41.79	1	41.79	116.44	0.0001
A^2	19.51	1	19.51	54.37	0.0007
B^2	2.10	1	2.10	5.86	0.0601
C^2	3.06	1	3.06	8.52	0.0331
Lack of fit	1.51	1	1.51	20.95	0.0102
Fit statistics					
Standard deviation	0.60				
Mean	87.65				
Coefficient of variation (%)	0.68				
R^2	0.9937				
Adjusted R^2	0.9823				
Adequate Precision	42.38				

Peer-reviewed version available at Catalysts 2020, 10, 190; doi:10.3390/catal10020190

The F-value of 87.33 and p value of 0.0001 indicate statistically significance of the process of the model. From Table 4, all the model terms are significant except CPK loading (B) and quadratic term of CPK loading (B^2). MeOH:HRNO has the highest significant effect on the honne-rubber seed-neem oil biodiesel (HRNOB) yield out of the three process input variables investigated. This implies that it has stronger effect on the HRNOB yield than both reaction time and CPK loading. The fitness of experimental data to a model can be explained by its R^2. R^2 of the model was evaluated as 0.9937, which signifies that the model could elucidate 99.37% of the variability [21]. For adequate precision, the required ratio should be > 4, for the value of 42.38 for the model indicates strong signal for the design purpose. Therefore, the design space can be directed by the model. Coefficient of variation (CV) is used to evaluate the capability of a model; a value < 10% indicates efficient model. The CV obtained for the model is 0.68%, which suggests that the model is capable of illustrating the process.

Figure 7a displays the plot of predicted HRNOB yields by the model versus the experimental HRNOB yields obtained in the laboratory. The predicted yields by the model are close in values to the experimental yields, which demonstrates the effectiveness of the model. It should be noted that the pure error in this model is insignificant within the range of process parameters investigated due to the near-alignment of experimental HRNOB yields and predicted HRNOB yields; which further confirms a good agreement between the model predicted yields and the experimental yields. Residual is a value between the experimental and predicted value. Hence, randomness of the experimental errors would make the residuals to follow a normal distribution [41]. Figure 7b shows a normal distribution of studentized residuals since it si a straight line and not S-shape curve [42]. Figure 7c shows the the plot of studentized residuals against model predicted HRNOB yields. The data points randomly scattered within the boundary, which may mean that the variation is consistent for all values of the response, an indication that the model is appropriate. The plot of outlier t for all experimental runs can be visualised as shown in Figure 7d. All the studentized residuals are within the ± 3.0 interval limit, demonstrating the fitness of the model. The diagnostic plots obtained this current study are similar to the ones reported for the modeling of transesterification process of neem-rubber seed oil blend with methanol over calcined elephant ear pod husk as catalyst [30]. Also, similar plots are reported for the model developed for the transesterification of soybean oil with ethanol using calcined waste cupuaçu seed as a solid catalyst [12].

Peer-reviewed version available at *Catalysts* **2020**, *10*, 190; doi:10.3390/catal10020190

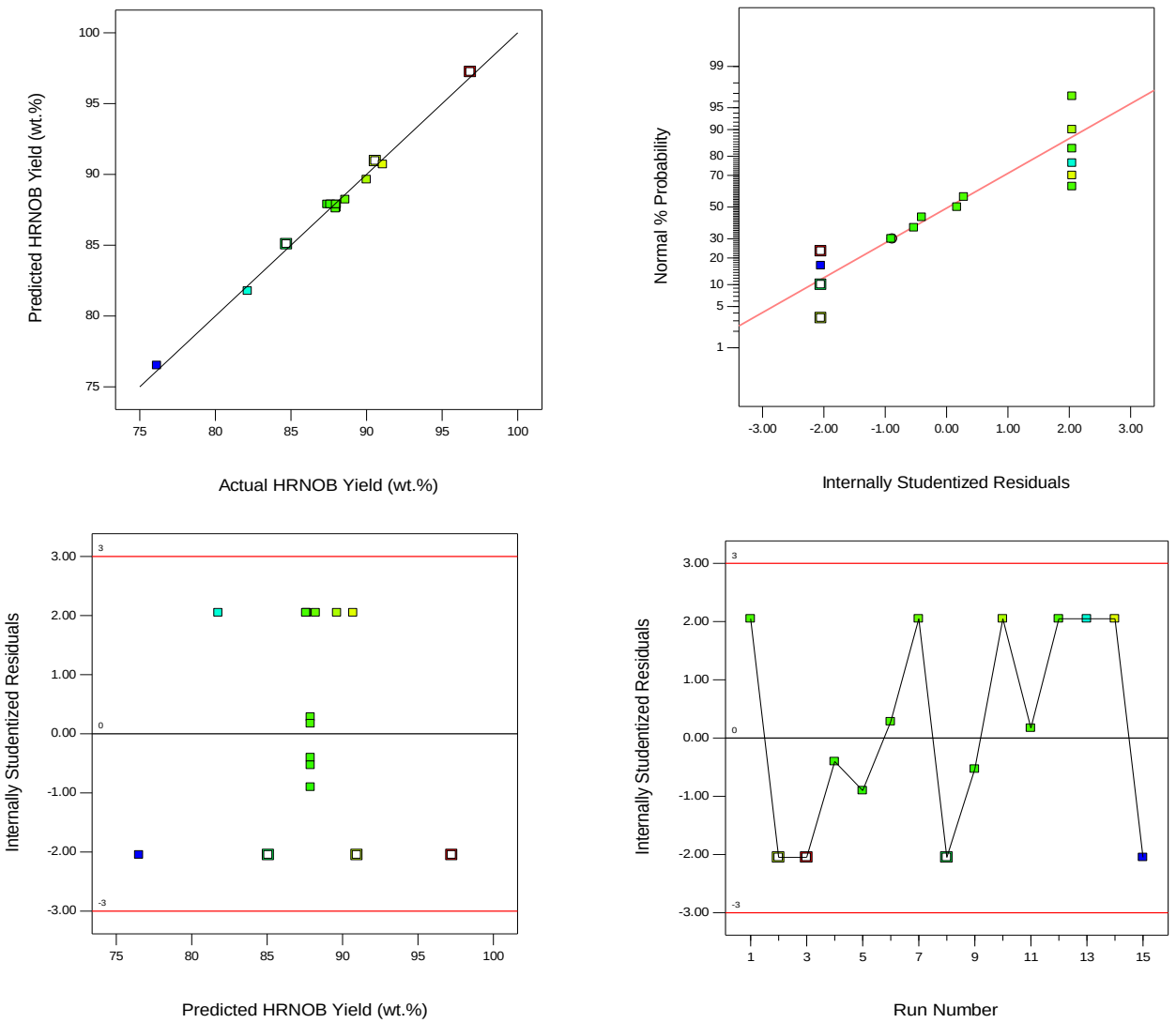

Figure 7. Diagnostic plots of the surface model for HRNOB synthesis.

Peer-reviewed version available at Catalysts 2020, 10, 190; doi:10.3390/catal10020190

2.5. Interactive effect of process parameters on HRNOB

Two-dimensional (contour) interactive effect of CPK loading and MeOH:HRNO while time was held constant is shown in Figure 8a. This plot reveals that at low CPK concentration, HRNOB yield increases with increase in MeOH:HRNO. Also, at high levels of both parameters, the plot reveals a direct relationship between CPK concentration and MeOH:HRNO which leads to high HRNOB yield. It has been shown that as the amount of catalyst increases, transesterification reaction accelerates due to attainment of equilibrium in shorter time [43]. Visual inspection of this plot could explain the reason the CPK loading is insignificant in the ANOVA results.

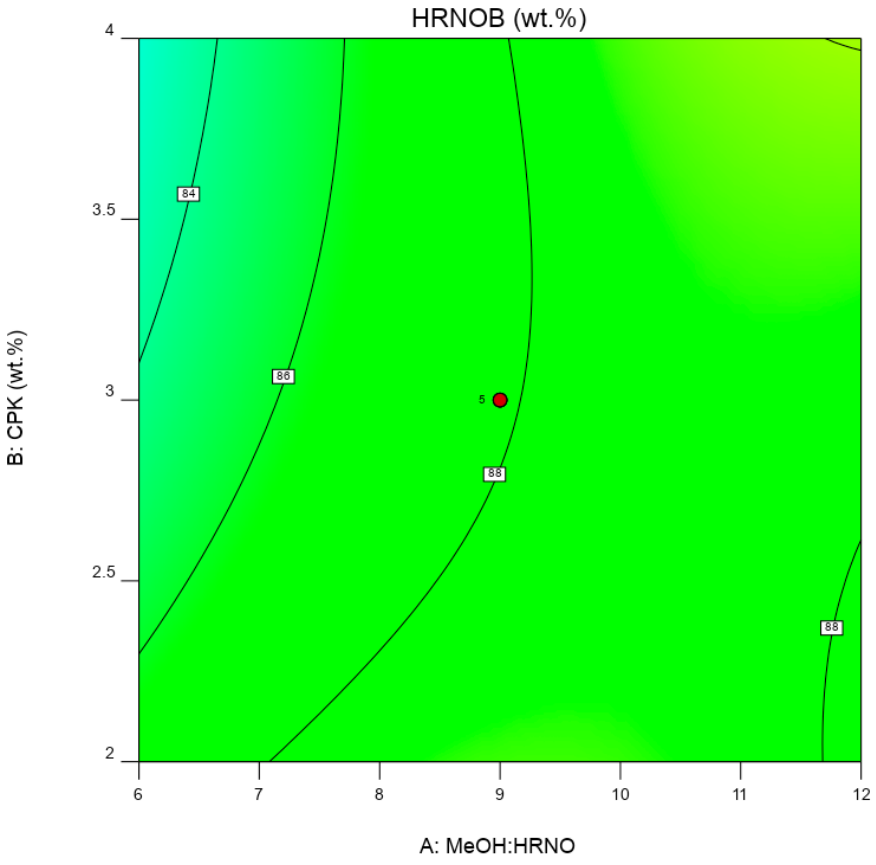

Figure 8a: Two-dimensional plot of CPK loading and MeOH:HRNO on HRNOB yield.

The two-dimensional plot of reaction time and CPK loading at constant MeOH:HRNO of 9:1 is shown in Figure 8b. From the plot, increase in CPK loading does not significantly increase the HRNOB yield with time. While HRNOB yield is maximum at the highest reaction time and lowest CPK amount, further increase in CPK concentration at that point leads to sharp reduction in biodiesel yield, though the HRNOB yield at high catalyst loading later increase with reduction in reaction time. The level of significance of reaction time could be attributed

Peer-reviewed version available at Catalysts 2020, 10, 190; doi:10.3390/catal10020190

to the effectiveness of microwave irradiation in aiding the conversion rate of the reactant mixture. Compared to conventional heating method, microwave irradiation within short time proved to be efficient in producing biodiesel. For instance, Nayak and Vyas [44] obtained biodiesel of 99.3% from papaya oil within 3.3 min when microwave was applied to the transesterification process. Similarly, biodiesel yield of 95.42% was observed within 388 s when transesterification of *Ceiba pentandra* oil was used under microwave-assisted transesterification [45]. In our study of rubber-neem oil blend, biodiesel yield of 98.77 ± 0.16 wt.% was observed through transesterification-aided with microwave within 5.88 min [30].

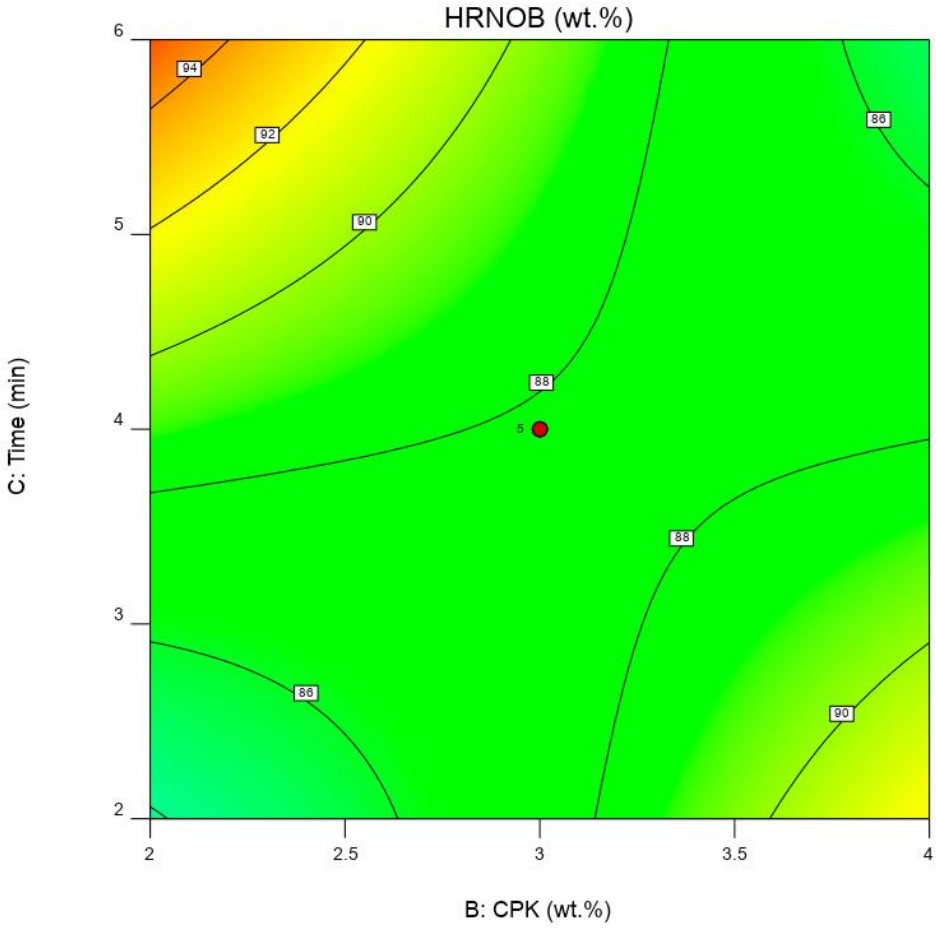

Figure 8b: Two-dimensional plot of CPK loading and time on HRNOB yield.

Figure 8c shows the interaction between time and MeOH:HRNO on HRNOB yield at constant CPK loading of 3 wt.%. In microwave-aided transesterification, reaction time has been shown to have significant effect on biodiesel yield [30, 46]. At low reaction time and low MeOH:HRNO, the biodiesel yield barely increased. This shows that enough time and high MeOH:HRNO are requirements for high biodiesel formation [7]. Thus, interaction of these two variables at the highest points increased the HRNOB yield. Both time and MeOH have been

Peer-reviewed version available at Catalysts 2020, 10, 190; doi:10.3390/catal10020190

demonstrated to influence biodiesel formation. MeOH level higher than what is required in terms of stochiometric is needed to drive the equilibrium reaction forward and at the same time, enough time is needed for the reaction to be completed. These observations have been reported in previous studies on transesterification reactions [12, 30, 44].

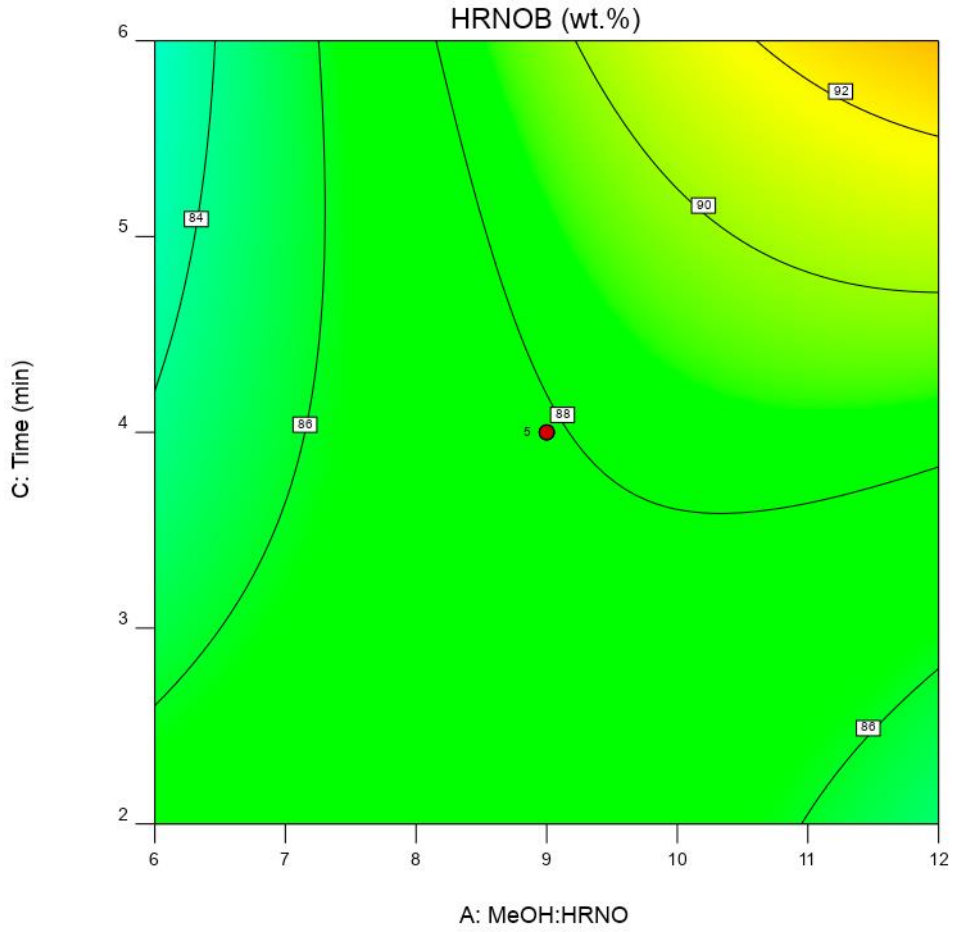

Figure 8c: Two-dimensional plot of time and MeOH:HRNO on HRNOB yield.

2.6. Optimization condition and model validation

The optimum values suggested for the three process input variables investigated in this study after solving the regression equation (Eq. 1) are MeOH:HRNO of 12:1, CPK of 1.158 wt.% and reaction time of 6 min with HRNOB yield predicted as 99 wt.% at desirability of 1.0. The optimal condition predicted was proved by validation experiment repeated three times. An average of 98.45 wt.% HRNOB yield was observed indicating that the model could accurately predict biodiesel yield. In a study of biodiesel synthesis using papaya oil and microwave-assisted transesterification, optimum biodiesel yield of 99.93 wt.% was obtained at NaOH loading of 0.95 wt.%, temperature of 62.33 ^{o}C, reaction time of 3.3 min and MeOH:oil ratio of

Peer-reviewed version available at Catalysts 2020, 10, 190; doi:10.3390/catal10020190

9.5:1 [44]. In another study involving blend of waste cooking oil and honne oil, it was shown that maximum biodiesel yield of 97.40 wt.% can be produced via microwave-aided transesterification using KOH concentration of 0.774 wt.%, stirring speed of 600 rpm, MeOH:oil of 59.60 vol.%, time of 7.15 min and at 100 ^{o}C [27]. Transesterification assisted with microwave was used to convert *Ceiba pentandra* oil to biodiesel with a maximum yield of 96.19%. using KOH concentration of 0.84%, stirring speed of 800 rpm, MeOH:oil of 60% and reaction time of 388 s [45]. In our previous study in which rubber seed and neem oils were blended and calcined ash of elephant ear pod husk was applied as a base catalyst, 98.77 wt.% biodiesel yield was achieved using optimal condition reaction time of 5.88 min, catalyst amount of 2.96 wt.% and MeOH:oil blend of 11.44:1 conducted under microwave irradiation [30]. The results of the current study showed that the CPK developed is effective and compared well with synthetic chemicals (KOH and NaOH) used as catalysts in other studies (Table 5).

The application of microwave irradiation in this present study helped reduced the reaction time significantly compared to the conventional heating via water bath or hotplate used for transesterification reaction. The typical reaction time reported in the conventional transesterification of some oils to biodiesel ranged between 25 min and 180 min [7, 13, 14, 18, 20, 21]. Microwave irradiation enhances transesterification reaction through a thermal effect and by evaporation of methanol [47]. The microwave interaction with the triglycerides and methanol results in a large reduction of activation energy due to increased interaction of triglycerides and methanol with the microwave irradiation which results in significant reduction of activation energy because of increased dipolar polarization. The choice of methanol over ethanol for the transesterification process in this current study is also helpful in the reduction of the reaction time used since methanol is a strong microwave absorber [47].

2.7. Quality of HRNOB

The characteristics of the HRNO and HRNOB were determined and compared with American and European standards (Table 6). Acid value of the HRNOB was within allowable limit, which means it can be used without causing corrosion in the internal combustion engine and other metal parts [48]. Flash point is the temperature at which biodiesel will ignite when exposed to flame [49]. Biodiesel produced in this study was well within the range specified. High flash point obtained may be due to the predominant presence of C18:1 and C18: 2 in the vegetable oil blend [50]. The cloud point of +12 ^{o}C and pour point of -6 ^{o}C of biodiesel produced in this study suggest that this fuel could be used successfully in cold weather areas.

Peer-reviewed version available at Catalysts 2020, 10, 190; doi:10.3390/catal10020190

Table 5. Review of mixed oils transesterification reaction conditions and yields.

Mixed oils	Nature of oils	Ratio	Catalyst	Transesterification condition	Yield	Ref
Cottonseed/castor	Both non-edible	50:50	NaOH	MeOH/oil/catalyst of 34:6:1	86%	[24]
Soybean/castor	Edible/non-edible	25:75	NaOH	MeOH/oil/catalyst of 34:6:1	87%	[24]
Palm oil/rubber seed	Edible/non-edible	50:50	KOH	64 ^{o}C, 1 h, catalyst of 1.3, MeOH:oil 6:1	97%	[25]
Pongamia/neem	Both non-edible	70:30	NaOH	60 – 65 ^{o}C, catalyst of 0.67%, MeOH:oil of 6:1 and 77 min,	86.2%	[26]
Waste cooking/honne	Waste/non-edible	70:30	KOH	100 ^{o}C, catalyst of 0.774 wt.%, 600 rpm, MeOH:oil of 59.60 vol.% and 7.15 min under microwave irradiation	97.65%	[27]
Pongamia/jatropha/honne	All are non-edible	1:1:1	KOH	64 ^{o}C, catalyst of 1.17w/v, oil:MeOH of 2.5 v/v and 95 min	98%	[28]
Soybean/rapeseed	Both edible	50:50	NaOH	55 ^{o}C, catalyst of 0.8 wt.%, MeOH:oil of 5:1 and 2 h	94%	[29]
Rubber seed/neem	Both non-edible	40:60	Calcined ash of elephant ear pod husk	150 W, MeOH:oil 11.44:1, catalyst of 2.96 wt.% and 5.88 min under microwave irradiation	98.77%	[30]
Castor/waste fish oil	Non-edible/waste	50:50	KOH	32 ^{o}C, catalyst of 0.5 wt.%, MeOH:oil of 8:1, 600 rpm and 30 min	95.2± 2.5%	[31]
Honne/rubber seed/neem	All are non-edible	1:1:1	Calcined CPK	150 W, MeOH:oil 12:1, catalyst of 1.158 wt.% and 6 min under microwave irradiation	98.45 wt.%	Present study

Peer-reviewed version available at Catalysts 2020, 10, 190; doi:10.3390/catal10020190

Table 6. Properties of HRNO, HRNOB and standards

Properties	Unit			Limit	
		HRNO	HRNOB	EN 14214	ASTM D6751
Density (15˚C)	kg/m^3	938	889	860 - 900	880
Acid value	mg KOH/g	31.97	0.45	0.5 max	0.5 max
FFA content	%	16.07	0.226	NS	NS
Kinematic viscosity	mm^2/s	66.15	4.89	3.5 - 5	1.9 - 6
Iodine value	g I_2/100g oil	81.89	44.9	< 120	NS
SV	mg KOH/g	206.17	190.74	NS	NS
Cetane number		51.34	64.8	51 min	47 min
Calorific Value	MJ/kg	39.75	40.94	35	NS
Pour Point	ºC	ND	-6	NS	-15 to 16
Flash point	ºC	ND	128	> 120	100 to 170
Cloud point	ºC	ND	12	NS	-3 to 12

NS = Not Specified, ND = Not Determined, SV = Saponification value

All parameters of the HRNOB were found to be within the prescribed standards. Thus, no modifications may be required in using this fuel in an existing diesel engine.

The IR spectral of HRNO and HRNOB are depicted in Figure 9 (a and b). Both spectral have similar peaks and the characteristics of the peaks are described in Table 7. The band around 3446 cm^{-1} is allocated to -C=O overtone. The region from 3009 – 2854 cm^{-1} indicates symmetric and asymetric streching vibration of the methyl group (-CH_3) [51]. The vibration at 2928 cm^{-1} is assigned to asymmetric CH_3 stretching. The well-known carbonyl peak 1750 – 1700 cm^{-1} has strong intensity in both spectral. Since no changes are obvious between 1650 and 1540 cm^{-1}, it shows no soap was present in the HRNOB [18, 52]. The fingerprint region (1300 – 900 cm^{-1}) which is recognized in oils are very distinct in both the spectral for HRNO and HRNOB [18, 52]. The rocking vibration is located in the region of 881 – 723 cm^{-1}. The presence of esters in both the HRNO and HRNOB are charaterized by the strong absorption of C=O streching frequency at 1743 cm^{-1} and by the strong absorption involving the streching of C-O near 1240 cm^{-1} [14, 18, 52, 53].

Peer-reviewed version available at *Catalysts* **2020**, *10*, 190; doi:10.3390/catal10020190

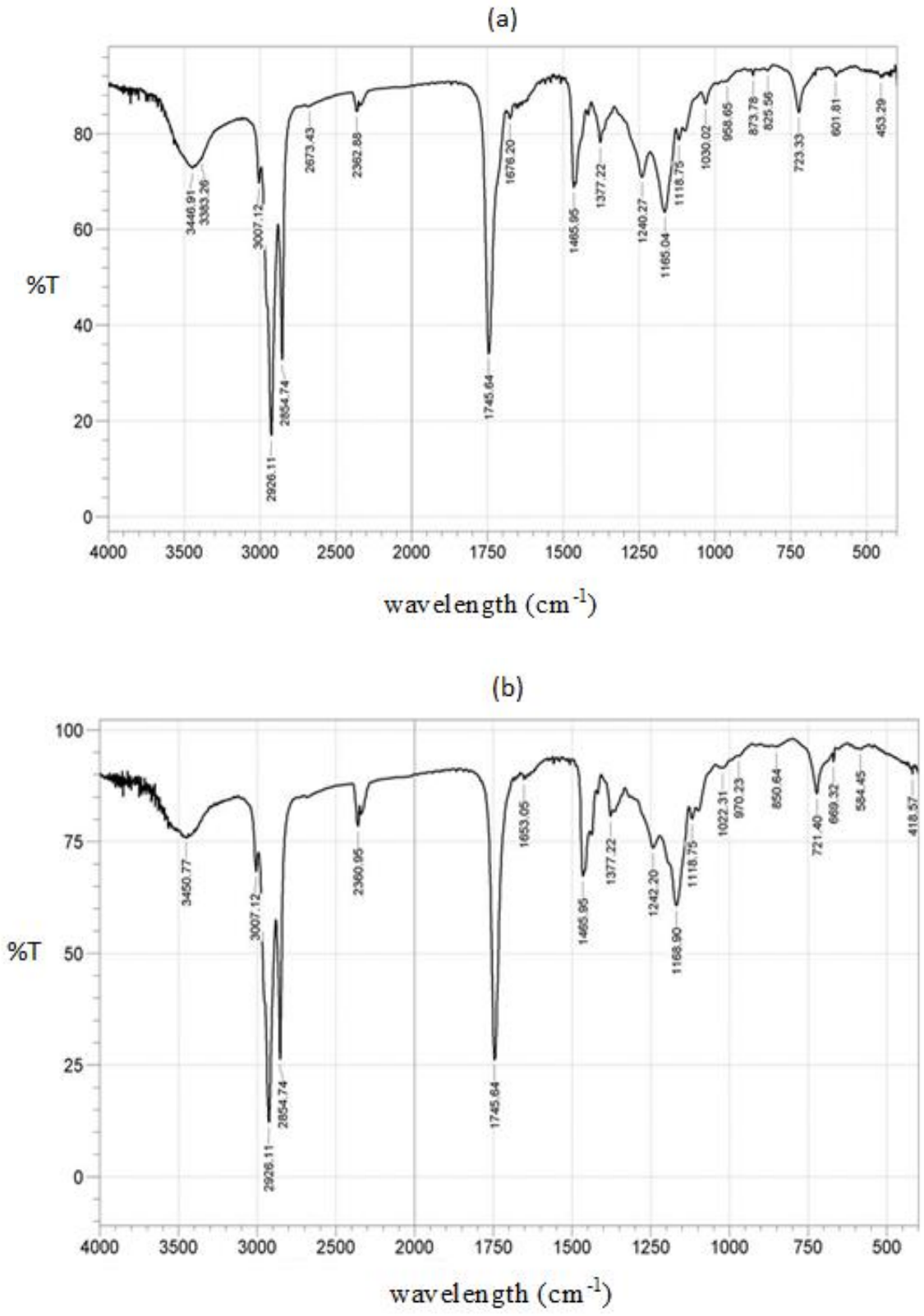

Figure 9. IR spectral; (a) HRNO and (b) HRNOB.

Peer-reviewed version available at Catalysts 2020, 10, 190; doi:10.3390/catal10020190

Table 7. Properties of absorption peaks for HRNO and HRNOB

Wavenumber (cm^{-1})	Functional group	Mode of vibration	Intensity	Reference
3450	-C=O	Overtone	Weak	[18, 53, 54]
3007	=C-H	Stretching	Strong	[29, 30, 55]
2926	-C-H (CH_2)	Asymmetric stretching vibration	Very strong	[14, 18, 54]
2854	-C-H (CH_2)	Symmetric stretching vibration	Very strong	[14, 18, 29]
1745	-C=O	Stretching	Very strong	[14, 18, 53]
1465	-CH_2	Shear-type vibration	Medium	[30, 53, 55]
1377	-CH_3	Bending vibration, symmetric deformation	Medium	[30, 53, 55]
1242	-CH_2	Stretching	Medium	[30, 55]
1168	C-O-C	Symmetric stretching vibration	strong	[14, 18, 29]
721	-CH_2	Bending out of plane, rocking vibration	Medium	[14, 18, 29]

Figure 10 shows the chromatogram of the HRNOB. The fatty acids of the HRNOB consist of total saturated methyl esters of 36.69%, which suggest improved oxidation stability and total unsaturated methyl esters of 63.51%, an indication that the biodiesel produced possessed excellent cold flow properties [56]. According to Table 8, monounsaturated fatty acid of oleic is the predominant contributor to the total unsaturated fatty acid methyl esters. The fatty acid composition of HRNOB is quite similar to the findings of previous studies in which biodiesel was produced from neem oil and neem-rubber oil blend [21, 30].

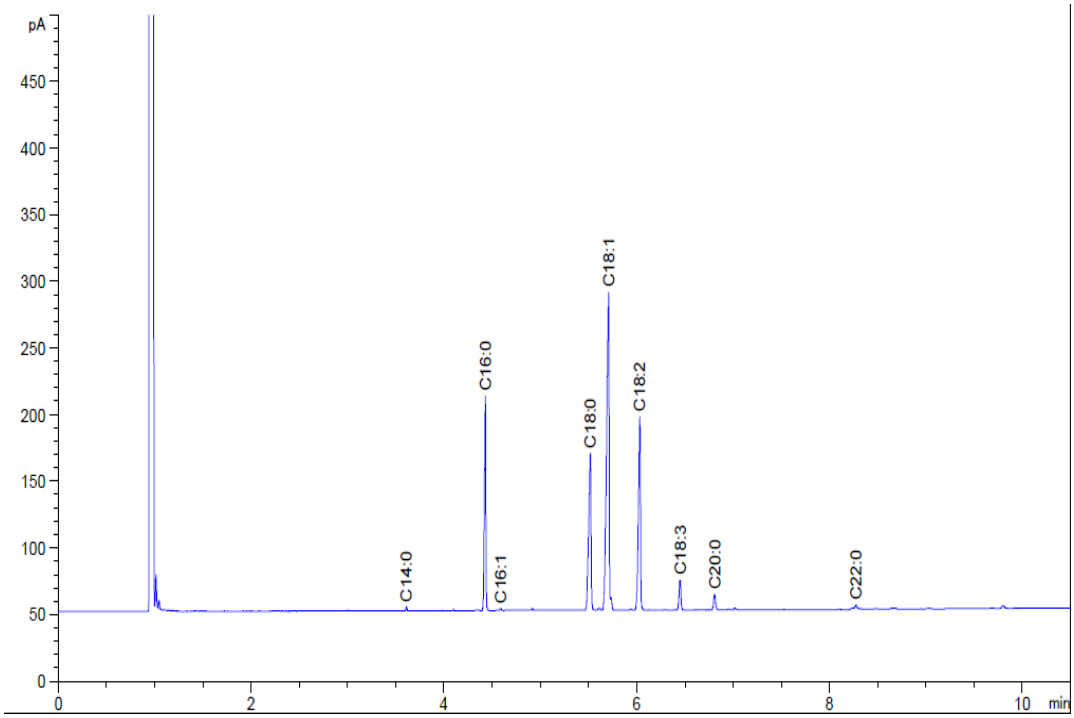

Figure 10. Chromatogram of HRNOB.

Peer-reviewed version available at Catalysts 2020, 10, 190; doi:10.3390/catal10020190

Table 8. Fatty acid profile of HRNOB

	Composition (%)			
	HRNOB	Honne	Rubber	Neem
Chain length	This study	Ong *et al*. [48]	Gimbun *et al*. [57]	Betiku *et al*. [58]
C14:0	0.22	0.1	-	-
C16:0	15.73	14.2	10.29	13.98
C16:1	0.12	0.3	-	0.39
C18:0	18.65	15.9	8.68	6.25
C18:1	40.42	39.8	20.07	45.00
C18:2	20.15	28.1	58.2	32.46
C18:3	2.84	0.2	0.8	0.6
C20:0	1.55	0.8	-	0.8
C22:0	0.54	-	-	0.5

2.8. Reusability study of CPK Catalyst

Reusability study of the calcined CPK was conducted at the optimized process condition and the results observed shown in Figure 11. On completion of each transesterification cycle, the product mixture and the catalyst were separated by centrifugation (8000 rpm for 10 min). The catalyst was reused without further treatment (no washing with acetone or calcination). At the end of the 4th cycle, calcined CPK was able to facilitate 89.46 wt.% biodiesel yield; hence, the calcined CPK demonstrated appreciable catalytic activity in its reutilization for transesterification. The reduction in the HRNOB yield after each cycle could be attributed to blockage of the catalyst active site and loss of part of the catalyst as well as leaching of active metals from the catalyst.

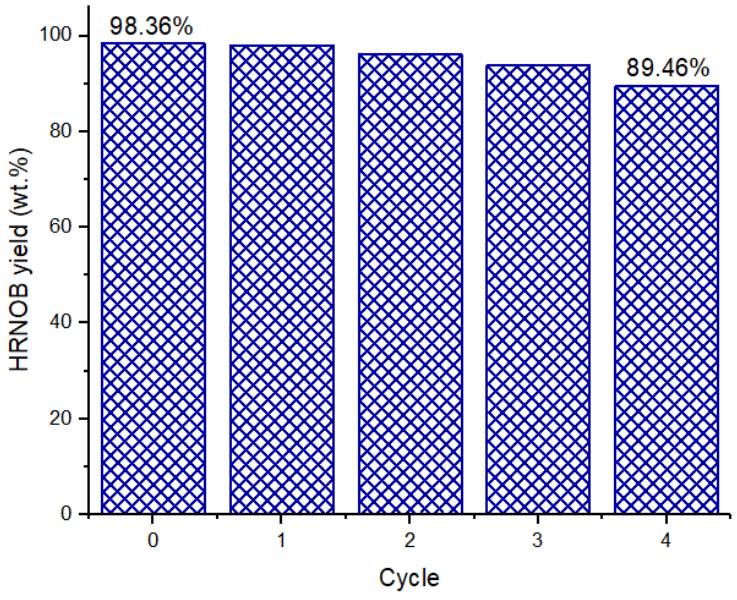

Figure 11. Reusability of calcined CPK at optimized condition

Peer-reviewed version available at Catalysts 2020, 10, 190; doi:10.3390/catal10020190

When *Brassica nigra* leaves calcined at 550 ^{o}C for 2 h was reused in the transesterification of soybean oil with methanol, the biodiesel yield reduced from 98.79% to 96% after the 3rd cycle [13]. The was a reduction of biodiesel yield from 95.23 % to 85.4% after 6th cycle of reuse of catalyst developed by calcination of *C. papaya* stem at 700 ^{o}C for 4 h [15]. In the case of calcined waste of cupuaçu seeds at 800 ^{o}C for 4 h, its reusability test showed that after the 3rd cycle, the biodiesel yield from soybean oil reduced from 98% to 22% [12]. We have previously reported that elephant ear pod husk calcined at 700 for 4 h can reused up to 4 times for transesterification of neem-rubber seed oil blend with a biodiesel yield reduction from 98.68% to 74.68% [30]. The reusability potential of the calcined CPK catalyst synthesized compared favourably with those cited in this work.

3. Experimental

3.1. Materials

Honne oil used for this study was extracted in the Biochemical Engineering laboratory, Obafemi Awolowo University, Ile-Ife, Nigeria. Rubber seed oil was procured from the Nigerian Rubber Research Institute, Edo State. Neem oil was purchased from the Nigerian National Research Institute for Chemical Technology, Kaduna State. Analytical grade reagents and chemicals were used in this study.

3.2. Preparation of CPK catalyst

CPK catalyst was developed from agrowastes; husk of cocoa pods, plantain peel and husk of kola nut pods. The plantain peels and cocoa pod husks used in this work were collected from a restaurant on the OAU campus and Aba Gbooro village, Ile-Ife, Nigeria, respectively while kola nut pod husks from a farm, Modakeke, Nigeria. First, each waste was separately sorted to remove dirt present. The agrowastes were cut into small pieces, thoroughly washed with municipal water and sundried for 2 weeks. The pieces of the agrowastes were further dried in an oven at 80 ^{o}C for 48 h to constant weight [22]. Then, the oven-dried agrowastes were completely combusted to produce ash individually. The resulting ashes were milled into powder in a porcelain mortar and pestle. The to synthesize the CPK, the three ashes from cocoa pod husk, plantain peel and kola nut pod husk were mixed in equal proportions. The ash mixture was heated in a muffle furnace at 300 - 1100 ^{o}C for 4 h [7, 22]. The heat-treated ash was ground to fine powder using porcelain mortar and pestle which was stored in a screwed bottle and kept in a desiccator for further analysis.

Peer-reviewed version available at Catalysts 2020, 10, 190; doi:10.3390/catal10020190

3.3. Characterization of synthesized CPK catalyst

The activity of the calcined CPK was analyzed to establish its suitability as a catalyst. The elemental composition and surface morphology of calcined CPK were analyzed with high resolution scanning electron microscope (AURIGA, Zeiss Germany) attached to the EDX spectroscopy. The diffraction pattern of calcined CPK was documented by an Advance Diffractometer -D8 (Bruker AXS, Karlsruhe, Germany) to observe the crystalline structure of the sample. The diffractometer was fitted out a LynxEye position sensitive detector employed with Cu Kα radiation source ($\lambda K_{\alpha 1}$ = 1.5406Å). Scanning of CPK was carried out in the region between 4.013º – 60.0152º in a continuous mode over 2-theta range. FTIR spectrometer was used to examine the active functional groups present at the active site of the calcined CPK. IR spectrum was recorded using KBr technique in a Thermo Nicolet iS10 FTIR spectrometer fitted with attenuated total reflectance (ATR) between 4000 and 400 cm^{-1} range. The pore structure and surface area of the calcined CPK was measured by BET method of physisorption of N_2 with Micromeritics Instrument (ASAP 2020, USA). Method of BJH was used to estimate total average pore size and pore volume of the calcined CPK [18, 23, 30].

3.4. Blending of honne, rubber seed and neem oils

The blending of honne oil, rubber seed oil and neem oil was done using a 1000-ml bottom flask following the method earlier described in our previous report [30]. The mixtures were prepared according to the following volumetric ratios: 20:60:20, 40:40:20, 60:20:20, 20:40:40, 40:20:40, 20:20:60 and 33.3:33.3:33.3 (Table 3). Prior to the blending, each oil was preheated at 60 ºC for 15 min. The preheated oils were blended together in a flask placed on a hot plate and stirred. Each blended oil was further heated at 60 ºC for 30 min on the on a hot plate with stirring to ensure uniform mixing. Physical and chemical properties of the individual oil and each oil blend were measured using the standard methods [59].

3.5. Model development for HRNO blend transesterification

In this study, CCRD design was used to model the transesterification of the oil blend with methanol using calcined CPK as the base catalyst. The range of independent variables investigated were MeOH:HRNO (6:1 - 12:1), CPK loading (2 - 4 wt.%) and reaction time (2 - 6 min) with the HRNOB yield as the response. A fractional factorial design with five-level-three-factor was applied to generate 15 set of experimental conditions carried out in batch-wise in a microwave device (Table 9). The axial distance α of each process variable was selected to

Peer-reviewed version available at Catalysts 2020, 10, 190; doi:10.3390/catal10020190

be 1.414 for orthogonality of the design and to test how repeatable the technique is, the center point was repeated five times. The experimental runs were randomized to reduce unexpected variation in the response. To connect the response and the independent variables, multiple regression model was used to fit the experimental data (Eq. 2). The characteristics of the quadratic model was assessed by various statistics. Optimum values of the process variables were determined with Design expert 10.0. The condition for optimum biodiesel yield was validated by performing experiment at optimum points of the design variables in triplicate.

$$R = \mu_o + \mu_1 A + \mu_2 B + \mu_3 C + \mu_{12} AB + \mu_{13} AC + \mu_{23} BC + \mu_{11} A^2 + \mu_{22} B^2 + \mu_{33} C^2 \quad (2)$$

where, R is the response (HRNOB yield), μ_o is the intercept term, μ_1, μ_2 and μ_3 are the coefficients of linear terms. μ_{12}, μ_{13}, and μ_{23} are coefficients of the interactive terms, μ_{11}, μ_{22} and μ_{33} are quadratic terms coefficients. A, B and C represent MeOH:HRNO, CPK loading and time, respectively.

Table 9. Experimental design for HRNOB synthesis

Run	MeOH:HRNO (*A*)	CPK (wt.%) (*B*)	Time (min) (*C*)
1	9	3	1.17157
2	12	4	2
3	12	2	6
4	9	3	4
5	9	3	4
6	9	3	4
7	9	4.41421	4
8	6	2	2
9	9	3	4
10	9	1.58579	4
11	9	3	4
12	13.2426	3	4
13	4.75736	3	4
14	9	3	6.82843
15	6	4	6

3.6. Esterification of HRNO blend

The HRNO blend (20:20:60) had an acid value of 31.97 mg KOH/g oil, which is too high for biodiesel synthesis. The pretreatment of this ternary oil blend was carried out in order to reduce the acid value in the oil blend to < 2 mg KOH/g oil [58]. The esterification process and the treatment of anhydrous ferric sulphate used as catalyst in this study are according to

Peer-reviewed version available at Catalysts 2020, 10, 190; doi:10.3390/catal10020190

Falowo *et al*. [30], which are as follows: temperature of 65 ^{o}C, reaction time 2 h, MeOH:oil blend of 25:1 and 10 wt.% ferric sulfate.

3.7. Transesterification of treated HRNO blend

Base catalyzed transesterification of the pretreated HRNO was carried out using a three-neck glass reactor of 500-ml capacity placed in a modified microwave device, SEVERIN Microwave with model number MW 7820. The microwave device was equipped with an external stirrer fitted with a Teflon rod with two blades and a reflux condenser system. The experiments were conducted as previously described following the experimental design in Table 9 [30]. For each experiment, the microwave device was set at 150 W and the reaction was performed at specified time according to CCRD. At the completion of the reaction, product mixture was centrifuged for 5 min at 8000 rpm. The biodiesel produced after separation was washed three times with distilled water warmed to 50 ^{o}C. The HRNOB yield from the HRNO was determined as described by Eq. (3). The quality of the biodiesel obtained was determined to ascertain its suitability as a fuel using methods earlier described our previous study [30].

$$\text{HRNOB yield} = \frac{\text{HRNOB produced (g)}}{\text{HRNO blend used (g)}} \times 100 \quad (3)$$

4. Conclusion

Blend of cocoa, plantain and kola nut wastes were used as precursors for catalyst synthesis. The characterization of the CPK catalyst obtained indicates that it could serves as heterogenous catalyst for transesterification reactions. Particularly, the presence of high level of K in the CPK makes it an alkaline biobase catalyst. Features of the CPK catalyst developed in this study indicate that it could provide sufficient accessibility to reactants in heterogenous catalyzed-transesterification reactions. Honne, rubber seed and neem oil blend containing volumetric ratio of 20:20:60 was converted to biodiesel by two-step transesterification process under microwave irradiation and catalyzed by the CPK. The optimum process parameters that gave maximum HRNOB yield of 98.45 wt.% are reaction time of 6 min, CPK loading of 1.158 wt.% and MeOH:oil blend of 12:1 under microwave irradiation. Analysis of fuel quality of the HRNOB produced satisfied the standards specified for biodiesel. Therefore, this study underscores possible use of mixture of agrowastes and blend of non-edible oils for biodiesel synthesis in sustainable manner. The HRNOB produced could be a potential replacement for diesel fuel either to be used directly or partially mixed with diesel fuel in diesel engines.

Peer-reviewed version available at *Catalysts* **2020**, *10*, 190; doi:10.3390/catal10020190

Acknowledgements

EB wishes to thank Tetfund for financial support for this work. The financial support of the Cape Peninsula University of Technology for this work is acknowledged by TVO.

References

[1]. Sahoo, P.; Das, L., Process optimization for biodiesel production from Jatropha, Karanja and Polanga oils. *Fuel* **2009,** 88, 1588-1594.
[2]. Knothe, G.; Razon, L.F., Biodiesel fuels. *Progress in Energy and Combustion Science* **2017,** 58, 36-59.
[3]. Thanh, L.T.; Okitsu, K.; Boi, L.V.; Maeda, Y., Catalytic technologies for biodiesel fuel production and utilization of glycerol: a review. *Catalysts* **2012,** 2, 191-222.
[4]. Abdullah, S.H.Y.S.; Hanapi, N.H.M.; Azid, A.; Umar, R.; Juahir, H.; Khatoon, H.; Endut, A., A review of biomass-derived heterogeneous catalyst for a sustainable biodiesel production. *Renewable and Sustainable Energy Reviews* **2017,** 70, 1040-1051.
[5]. Leung, D.Y.C.; Wu, X.; Leung, M.K.H., A review on biodiesel production using catalyzed transesterification. *Applied Energy* **2010,** 87, 1083-1095.
[6]. Semwal, S.; Arora, A.K.; Badoni, R.P.; Tuli, D.K., Biodiesel production using heterogeneous catalysts. *Bioresource technology* **2011,** 102, 2151-61.
[7]. Betiku, E.; Akintunde, A.M.; Ojumu, T.V., Banana peels as a biobase catalyst for fatty acid methyl esters production using Napoleon's plume (Bauhinia monandra) seed oil: A process parameters optimization study. *Energy* **2016,** 103, 797-806.
[8]. Boey, P.-L.; Maniam, G.P.; Hamid, S.A.; Ali, D.M.H., Utilization of waste cockle shell (Anadara granosa) in biodiesel production from palm olein: optimization using response surface methodology. *Fuel* **2011,** 90, 2353-2358.
[9]. Odude, V.O.; Adesina, A.J.; Oyetunde, O.O.; Adeyemi, O.O.; Ishola, N.B.; Etim, A.O.; Betiku, E., Application of Agricultural Waste-Based Catalysts to Transesterification of Esterified Palm Kernel Oil into Biodiesel: A Case of Banana Fruit Peel Versus Cocoa Pod Husk. *Waste and Biomass Valorization* **2017**, 1-12.
[10]. Liu, D.; Seeburg, D.; Kreft, S.; Bindig, R.; Hartmann, I.; Schneider, D.; Enke, D.; Wohlrab, S., Rice Husk Derived Porous Silica as Support for Pd and CeO2 for Low Temperature Catalytic Methane Combustion. *Catalysts* **2019,** 9, 26.
[11]. Nisar, J.; Razaq, R.; Farooq, M.; Iqbal, M.; Khan, R.A.; Sayed, M.; Shah, A.; ur Rahman, I., Enhanced biodiesel production from Jatropha oil using calcined waste animal bones as catalyst. *Renew Energy* **2017,** 101, 111-119.
[12]. Mendonça, I.M.; Machado, F.L.; Silva, C.C.; Junior, S.D.; Takeno, M.L.; de Sousa Maia, P.J.; Manzato, L.; de Freitas, F.A., Application of calcined waste cupuaçu (Theobroma grandiflorum) seeds as a low-cost solid catalyst in soybean oil ethanolysis: Statistical optimization. *Energ Convers Manage* **2019,** 200, 112095.
[13]. Nath, B.; Das, B.; Kalita, P.; Basumatary, S., Waste to value addition: Utilization of waste Brassica nigra plant derived novel green heterogeneous base catalyst for effective synthesis of biodiesel. *J Clean Prod* **2019,** 239, 118112.
[14]. Balajii, M.; Niju, S., Banana peduncle–A green and renewable heterogeneous base catalyst for biodiesel production from Ceiba pentandra oil. *Renew Energy* **2020,** 146, 2255-2269.
[15]. Gohain, M.; Laskar, K.; Paul, A.K.; Daimary, N.; Maharana, M.; Goswami, I.K.; Hazarika, A.; Bora, U.; Deka, D., Carica papaya stem: A source of versatile heterogeneous catalyst for biodiesel production and C–C bond formation. *Renew Energy* **2020,** 147, 541-555.

Peer-reviewed version available at *Catalysts* **2020**, *10*, 190; doi:10.3390/catal10020190

[16]. Pathak, G.; Das, D.; Rajkumari, K.; Rokhum, L., Exploiting waste: towards a sustainable production of biodiesel using Musa acuminata peel ash as a heterogeneous catalyst. *Green Chemistry* **2018,** 20, 2365-2373.

[17]. Adeyi, O., Proximate composition of some agricultural wastes in Nigeria and their potential use in activated carbon production. *Journal of Applied Sciences and Environmental Management* **2010,** 14.

[18]. Betiku, E.; Okeleye, A.A.; Ishola, N.B.; Osunleke, A.S.; Ojumu, T.V., Development of a Novel Mesoporous Biocatalyst Derived from Kola Nut Pod Husk for Conversion of Kariya Seed Oil to Methyl Esters: A Case of Synthesis, Modeling and Optimization Studies. *Catalysis Letters* **2019,** 149, 1772-1787.

[19]. Osakwe, E.; Ani, I.; Akpan, U.; Olutoye, M. In *Kolanut pod husk as a biobase catalyst for fatty acid methyl ester production using Thevetia peruviana (Yellow oleander) seed oil*, IOP Conference Series: Earth and Environmental Science, 2018; IOP Publishing: 2018; p 012008.

[20]. Ofori-Boateng, C.; Lee, K.T., The potential of using cocoa pod husks as green solid base catalysts for the transesterification of soybean oil into biodiesel: Effects of biodiesel on engine performance. *Chem Eng J* **2013,** 220, 395-401.

[21]. Betiku, E.; Etim, A.O.; Pereao, O.; Ojumu, T.V., Two-step conversion of neem (Azadirachta indica) seed oil into fatty methyl esters using an heterogeneous biomass-based catalyst: An example of cocoa pod husk. *Energy and Fuels* **2017,** 31, 6182–6193

[22]. Betiku, E.; Ajala, S.O., Modeling and optimization of Thevetia peruviana (yellow oleander) oil biodiesel synthesis via Musa paradisiacal (plantain) peels as heterogeneous base catalyst: A case of artificial neural network vs. response surface methodology. *Ind Crops Prods* **2014,** 53, 314-322.

[23]. Etim, A.O.; Betiku, E.; Ajala, S.O.; Olaniyi, P.J.; Ojumu, T.V., Potential of Ripe Plantain Fruit Peels as an Ecofriendly Catalyst for Biodiesel Synthesis: Optimization by Artificial Neural Network Integrated with Genetic Algorithm. *Sustainability* **2018,** 10, 707.

[24]. Meneghetti, S.M.P.; Meneghetti, M.R.; Serra, T.M.; Barbosa, D.C.; Wolf, C.R., Biodiesel production from vegetable oil mixtures: cottonseed, soybean, and castor oils. *Energy Fuels* **2007,** 21, 3746-3747.

[25]. Khalil, I.; Aziz, A.R.A.; Yusup, S.; Heikal, M.; El-Adawy, M., Response surface methodology for the optimization of the production of rubber seed/palm oil biodiesel, IDI diesel engine performance, and emissions. *Biomass Conversion and Biorefinery* **2017,** 7, 37-49.

[26]. Vinayaka, A.S.; Mahanty, B.; Rene, E.R.; Behera, S.K., Biodiesel production by transesterification of a mixture of pongamia and neem oils. *Biofuels* **2018**, 1-9.

[27]. Milano, J.; Ong, H.C.; Masjuki, H.; Silitonga, A.; Chen, W.-H.; Kusumo, F.; Dharma, S.; Sebayang, A., Optimization of biodiesel production by microwave irradiation-assisted transesterification for waste cooking oil-Calophyllum inophyllum oil via response surface methodology. *Energ Convers Manage* **2018,** 158, 400-415.

[28]. Miraculas, G.A.; Bose, N.; Raj, R.E., Process parameter optimization for biodiesel production from mixed feedstock using empirical model. *Sustainable Energy Technologies and Assessments* **2018,** 28, 54-59.

[29]. Qiu, F.; Li, Y.; Yang, D.; Li, X.; Sun, P., Biodiesel production from mixed soybean oil and rapeseed oil. *Appl Energy* **2011,** 88, 2050-2055.

[30]. Falowo, O.A.; Oloko-Oba, M.I.; Betiku, E., Biodiesel production intensification via microwave irradiation-assisted transesterification of oil blend using nanoparticles from elephant-ear tree pod husk as a base heterogeneous catalyst. *Chemical Engineering and Processing-Process Intensification* **2019,** 140, 157-170.

Peer-reviewed version available at *Catalysts* **2020**, *10*, 190; doi:10.3390/catal10020190

[31]. Fadhil, A.B.; Al-Tikrity, E.T.; Albadree, M.A., Biodiesel production from mixed non-edible oils, castor seed oil and waste fish oil. *Fuel* **2017,** 210, 721-728.
[32]. Sharma, M.; Khan, A.A.; Puri, S.; Tuli, D., Wood ash as a potential heterogeneous catalyst for biodiesel synthesis. *Biomass Bioenergy* **2012,** 41, 94-106.
[33]. Lukić, I.; Krstić, J.; Jovanović, D.; Skala, D., Alumina/silica supported K 2 CO 3 as a catalyst for biodiesel synthesis from sunflower oil. *Bioresour Technol* **2009,** 100, 4690-4696.
[34]. Sharma, M.; Khan, A.A.; Puri, S.K.; Tuli, D.K., Wood ash as a potential heterogeneous catalyst for biodiesel synthesis. *Biomass and Bioenergy* **2012,** 41, 94-106.
[35]. Sing, K.; Everett, D.; Haul, R.; Moscou, L.; Pierotti, L.; Rouquerol, J.; Siemieniewska, T., International union of pure and applied chemistry physical chemistry division reporting physisorption data for gas/soils systems with special reference to the determination of surface area and porosity. *Pure Appl Chem* **1985,** 57, 603-619.
[36]. Deshmane, V.G.; Adewuyi, Y.G., Mesoporous nanocrystalline sulfated zirconia synthesis and its application for FFA esterification in oils. *Applied Catalysis A: General* **2013,** 462, 196-206.
[37]. Storck, S.; Bretinger, H.; Maier, W.F., Characterization of micro-and mesoporous solids by physisorption methods and pore-size analysis. *Applied Catalysis A: General* **1998,** 174, 137-146.
[38]. Knothe, G., Dependence of biodiesel fuel properties on the structure of fatty acid alkyl esters. *Fuel processing technology* **2005,** 86, 1059-1070.
[39]. Demirbaş, A., Relationships derived from physical properties of vegetable oil and biodiesel fuels. *Fuel* **2008,** 87, 1743-1748.
[40]. Wang, Y.; Ou, S.; Liu, P.; Zhang, Z., Preparation of biodiesel from waste cooking oil via two-step catalyzed process. *Energy conversion and management* **2007,** 48, 184-188.
[41]. Hamidreza, J.; Nor, A.; Amin, T.-k.; Noshadi, I., Microwave assisted biodiesel production from Jatropha curcas L. seed by two-step in situ process: optimization using response surface methodology. *Bioresource technology* **2013,** 136, 565-573.
[42]. Körbahti, B.K.; Rauf, M., Response surface methodology (RSM) analysis of photoinduced decoloration of toludine blue. *Chemical Engineering Journal* **2008,** 136, 25-30.
[43]. Tan, Y.H.; Abdullah, M.O.; Nolasco-Hipolito, C.; Zauzi, N.S.A., Application of RSM and Taguchi methods for optimizing the transesterification of waste cooking oil catalyzed by solid ostrich and chicken-eggshell derived CaO. *Renewable Energy* **2017,** 114, 437-447.
[44]. Nayak, M.G.; Vyas, A.P., Optimization of microwave-assisted biodiesel production from Papaya oil using response surface methodology. *Renew Energy* **2019,** 138, 18-28.
[45]. Silitonga, A.; Shamsuddin, A.; Mahlia, T.; Milano, J.; Kusumo, F.; Siswantoro, J.; Dharma, S.; Sebayang, A.; Masjuki, H.; Ong, H.C., Biodiesel synthesis from Ceiba pentandra oil by microwave irradiation-assisted transesterification: ELM modeling and optimization. *Renew Energy* **2020,** 146, 1278-1291.
[46]. Hsiao, M.-C.; Lin, C.-C.; Chang, Y.-H., Microwave irradiation-assisted transesterification of soybean oil to biodiesel catalyzed by nanopowder calcium oxide. *Fuel* **2011,** 90, 1963-1967.
[47]. Gude, V.G.; Patil, P.; Martinez-Guerra, E.; Deng, S.; Nirmalakhandan, N., Microwave energy potential for biodiesel production. *Sustainable Chemical Processes* **2013,** 1, 5.
[48]. Ong, H.C.; Masjuki, H.; Mahlia, T.; Silitonga, A.; Chong, W.; Leong, K., Optimization of biodiesel production and engine performance from high free fatty acid Calophyllum inophyllum oil in CI diesel engine. *Energy Conversion and Management* **2014,** 81, 30-40.

[49]. Atabani, A.E.; Silitonga, A.S.; Badruddin, I.A.; Mahlia, T.; Masjuki, H.; Mekhilef, S., A comprehensive review on biodiesel as an alternative energy resource and its characteristics. *Renewable and sustainable energy reviews* **2012,** 16, 2070-2093.

[50]. Sanford, S.D.; White, J.; Shah, P.; Wee, C.; Valverde, M.; Meier, G., Feedstock and Biodiesel Characteristics Report–2009. *Renewable Energy Group* **2010**.

[51]. Rabelo, S.N.; Ferraz, V.P.; Oliveira, L.S.; Franca, A.S., FTIR analysis for quantification of fatty acid methyl esters in biodiesel produced by microwave-assisted transesterification. *International Journal of Environmental Science and Development* **2015,** 6, 964.

[52]. Soares, I.P.; Rezende, T.F.; Silva, R.C.; Castro, E.V.R.; Fortes, I.C., Multivariate calibration by variable selection for blends of raw soybean oil/biodiesel from different sources using fourier transform infrared spectroscopy (FTIR) spectra data. *Energy Fuels* **2008,** 22, 2079-2083.

[53]. Guillén, M.D.; Cabo, N., Relationships between the Composition of Edible Oils and Lard and the Ratio of the Absorbance of Specific Bands of Their Fourier Transform Infrared Spectra. Role of Some Bands of the Fingerprint Region. *Journal of Agricultural & Food Chemistry* **1998,** 46, 1788-1793.

[54]. Oladipo, B.; Betiku, E., Process optimization of solvent extraction of seed oil from Moringa oleifera: An appraisal of quantitative and qualitative process variables on oil quality using D-optimal design. *Biocatalysis and Agricultural Biotechnology* **2019**, 101187.

[55]. Latchubugata, C.S.; Kondapaneni, R.V.; Patluri, K.K.; Virendra, U.; Vedantam, S., Kinetics and Optimization Studies using Response Surface Methodology in Biodiesel Production using Heterogeneous Catalyst. *Chemical Engineering Research and Design* **2018,** 135, 129–139.

[56]. Dharma, S.; Masjuki, H.H.; Ong, H.C.; Sebayang, A.H.; Silitonga, A.S.; Kusumo, F.; Mahlia, T.M.I., Optimization of biodiesel production process for mixed Jatropha curcas–Ceiba pentandra biodiesel using response surface methodology. *Energy Conversion and Management* **2016,** 115, 178-190.

[57]. Gimbun, J.; Ali, S.; Kanwal, C.; Shah, L.A.; Ghazali, N.H.M.; Cheng, C.K.; Nurdin, S., Biodiesel production from rubber seed oil using a limestone based catalyst. *Advances in Materials Physics and Chemistry* **2012,** 2, 138-141.

[58]. Betiku, E.; Omilakin, O.R.; Ajala, S.O.; Okeleye, A.A.; Taiwo, A.E.; Solomon, B.O., Mathematical modeling and process parameters optimization studies by artificial neural network and response surface methodology: A case of non-edible neem (Azadirachta indica) seed oil biodiesel synthesis. *Energy* **2014,** 72, 266-273.

[59]. AOAC, Official methods of analysis of the Association of Official Analytical Chemists. Official methods of analysis of the Association of Official Analytical Chemists. In 1990.